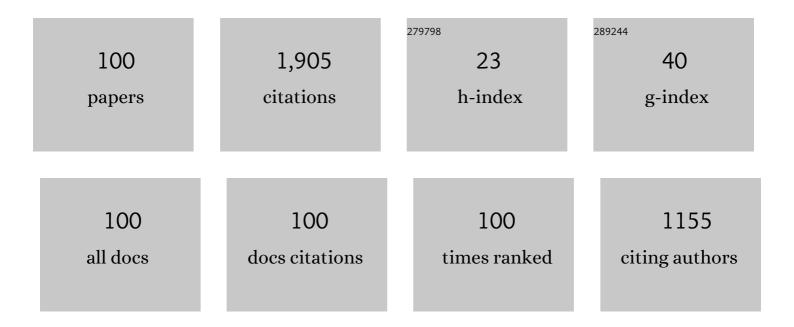
List of Publications by Year in descending order

Source: https://exaly.com/author-pdf/3155306/publications.pdf Version: 2024-02-01



#	Article	IF	CITATIONS
1	Integrated Waveguide Grating Vortex Laser Generator Directly Written in Nd:YAG Crystal. IEEE Photonics Technology Letters, 2022, 34, 409-412.	2.5	4
2	Two-Axis Bending Sensor Based on Asymmetric Grid Long-Period Fiber Grating. IEEE Sensors Journal, 2022, 22, 10567-10575.	4.7	9
3	Efficient Switchable Common Path Interferometer for Transmission Matrix Characterization of Scattering Medium. IEEE Photonics Journal, 2022, 14, 1-5.	2.0	0
4	Ultrasensitive Fabry–Perot Strain Sensor Based on Vernier Effect and Tapered FBG-in-Hollow Silica Tube. IEEE Sensors Journal, 2021, 21, 3035-3041.	4.7	20
5	Arc Radius-Chirped Long-Period Fiber Grating by High Frequency COâ,,-Laser Writing. IEEE Photonics Technology Letters, 2021, 33, 499-502.	2.5	4
6	7-Ring-Air-Core Trench-Assisted Fibre Supporting >300 Radially Fundamental OAM Modes Across S+C+L Bands. , 2021, , .		0
7	High-sensitivity bending vector sensor based on Î <sup>3</sup> -shaped long-period fiber grating. Optics and Laser Technology, 2021, 142, 107255.	4.6	18
8	ÂRapid Mode Decomposition of Few-Mode Fiber By Artificial Neural Network. Journal of Lightwave Technology, 2021, 39, 6294-6300.	4.6	15
9	Air-Core Non-Zero Dispersion-Shifted Fiber With High-Index Ring for OAM Mode. IEEE Access, 2021, 9, 107804-107811.	4.2	2
10	High sensitivity optical fiber temperature sensor based on PDMS-filled with extended measuring range. Optik, 2021, 248, 168181.	2.9	4
11	Simultaneous Measurement of Curvature Vector and Temperature Based on Composite Gratings Inscribed on D-Shaped Fiber. IEEE Sensors Journal, 2021, 21, 25758-25766.	4.7	11
12	Ultra-high sensitivity and temperature-compensated Fabry–Perot strain sensor based on tapered FBG. Optics and Laser Technology, 2020, 124, 105997.	4.6	30
13	Ultra-Compact Optical Thermo-Hygrometer Based on Bilayer Micro-Cap on Fiber Facet. IEEE Photonics Technology Letters, 2020, 32, 1089-1092.	2.5	3
14	Two-Octave Supercontinuum Generation of High-Order OAM Modes in Air-Core Asâ,,Sâ,ƒ Ring Fiber. IEEE Access, 2020, 8, 114135-114142.	4.2	15
15	Simultaneous Measurement of RI and Temperature Based on Compact U-Shaped Interferometer. IEEE Sensors Journal, 2020, 20, 3593-3598.	4.7	18
16	Highly dispersive coupled ring-core fiber for orbital angular momentum modes. Applied Physics Letters, 2020, 117, .	3.3	13
17	High-sensitivity temperature sensor based on ethanol-sealed double helix microfiber coupler. Optical Engineering, 2020, 59, 1.	1.0	2
18	Temperature self-compensation strain sensor based on cascaded concave-lens-like long-period fiber gratings. Applied Optics, 2020, 59, 2352,	1.8	3

#	Article	IF	CITATIONS
19	Parallelized fiber Michelson interferometers with advanced curvature sensitivity plus abated temperature crosstalk. Optics Letters, 2020, 45, 4996.	3.3	24
20	Two-dimensional microbend sensor based on the 2-core fiber with hump-shaped taper fiber structure. Optical Fiber Technology, 2019, 52, 101948.	2.7	9
21	Lab-on-tip: Protruding-shaped all-fiber plasmonic microtip probe toward in-situ chem-bio detection. Sensors and Actuators B: Chemical, 2019, 301, 127128.	7.8	13
22	Micro-Cap on 2-Core-Fiber Facet Hybrid Interferometer for Dual-Parameter Sensing. Journal of Lightwave Technology, 2019, 37, 6114-6120.	4.6	11
23	Ultra-high sensitivity liquid level sensor based on CO2 laser local refractive index curved modulation effect. Optics and Laser Technology, 2019, 120, 105755.	4.6	6
24	Tunable Autler–Townes Splitting in Optical Fiber. Journal of Lightwave Technology, 2019, 37, 3620-3625.	4.6	2
25	High-Sensitivity Gas Pressure Fabry–Perot Fiber Probe With Micro-Channel Based on Vernier Effect. Journal of Lightwave Technology, 2019, 37, 3444-3451.	4.6	68
26	Parabolic-cylinder-like long-period fiber grating sensor based on refractive index modulation enhancement effect. Applied Optics, 2019, 58, 1772.	1.8	11
27	Torsion bidirectional sensor based on tilted-arc long-period fiber grating. Optics Express, 2019, 27, 37695.	3.4	16
28	Protruding-shaped SiO2-microtip: from fabrication innovation to microphotonic device construction. Optics Letters, 2019, 44, 3514.	3.3	3
29	Optical screwdriving induced by the quantum spin Hall effect of surface plasmons near an interface between strongly chiral material and air. Physical Review A, 2018, 97, .	2.5	9
30	Bending Vector Sensing Based on Arch-Shaped Long-Period Fiber Grating. IEEE Sensors Journal, 2018, 18, 3125-3130.	4.7	24
31	Temperature-Independent Micro-Refractometer Based on Cascaded In-Fiber Air Cavities With Strain-Error Correction. IEEE Sensors Journal, 2018, 18, 8773-8780.	4.7	6
32	Two-axis bending vector sensor based on a long-period fiber grating cascading with a hump-shaped taper. Measurement Science and Technology, 2018, 29, 095107.	2.6	10
33	Microcavity-coupled fiber Bragg grating with tunable reflection spectra and speed of light. Optics Letters, 2018, 43, 1662.	3.3	5
34	V-Shaped Long-Period Fiber Grating High-Sensitive Bending Vector Sensor. IEEE Photonics Technology Letters, 2018, 30, 1531-1534.	2.5	21
35	Helical Fiber Interferometer Using Flame-Heated Treatment for Torsion Sensing Application. IEEE Photonics Technology Letters, 2017, 29, 161-164.	2.5	10
36	Two-Dimensional Bending Vector Sensor Based on the Multimode-3-Core-Multimode Fiber Structure. IEEE Photonics Technology Letters, 2017, 29, 822-825.	2.5	30

#	Article	IF	CITATIONS
37	Bending Vector Sensor Based on a Pair of Opposite Tilted Long-Period Fiber Gratings. IEEE Photonics Technology Letters, 2017, 29, 224-227.	2.5	40
38	2-D Medium–High Frequency Fiber Bragg Gratings Accelerometer. IEEE Sensors Journal, 2017, 17, 614-618.	4.7	36
39	Torsion sensor based on two cascaded long period fiber gratings fabricated by CO2 laser pulse irradiation and HF etching technique respectively. Journal of Modern Optics, 2017, 64, 541-545.	1.3	8
40	Realizing torsion detection using berry phase in an angle-chirped long-period fiber grating. Optics Express, 2017, 25, 13448.	3.4	21
41	Two-dimensional microbend sensor based on long-period fiber gratings in an isosceles triangle arrangement three-core fiber. Optics Letters, 2017, 42, 4938.	3.3	53
42	Concave-lens-like long-period fiber grating bidirectional high-sensitivity bending sensor. Optics Letters, 2017, 42, 3892.	3.3	49
43	Ringing phenomenon in chaotic microcavity for high-speed ultra-sensitive sensing. Scientific Reports, 2016, 6, 38922.	3.3	4
44	In-line polarization rotator based on the quantum-optical analogy. Optics Letters, 2016, 41, 2113.	3.3	3
45	Bending Vector Sensor Based on the Multimode-2-Core-Multimode Fiber Structure. IEEE Photonics Technology Letters, 2016, , 1-1.	2.5	23
46	Bending vector sensor based on Mach–Zehnder interferometer using S type fibre taper and lateral-offset. Journal of Modern Optics, 2016, 63, 2146-2150.	1.3	14
47	Mach–Zehnder Interferometer Based on Interference of Selective High-Order Core Modes. IEEE Photonics Technology Letters, 2016, 28, 71-74.	2.5	28
48	Bidirectional Torsion Sensor Based on a Pair of Helical Long-Period Fiber Gratings. IEEE Photonics Technology Letters, 2016, 28, 1700-1702.	2.5	37
49	Mechanism and characteristics of asymmetrically phase-shifted corrugated long-period fiber grating fabricated by burning fiber coating and etching cladding technology. Journal of Modern Optics, 2015, 62, 584-587.	1.3	4
50	CO <sub>2</sub> -Laser-Induced Long Period Fiber Gratings in Few Mode Fibers. IEEE Photonics Technology Letters, 2015, 27, 145-148.	2.5	66
51	Temperature-Independent Force Sensor Based on PSLPFG Induced by Electric-Arc Discharge. IEEE Photonics Technology Letters, 2015, 27, 1946-1948.	2.5	9
52	Bending Vector Sensor Based on a Sector-Shaped Long-Period Grating. IEEE Photonics Technology Letters, 2015, 27, 713-716.	2.5	70
53	Two-dimensional bending vector sensor based on Mach-Zehnder interferometer of two orthogonal lateral-offsets. Microwave and Optical Technology Letters, 2015, 57, 709-713.	1.4	12
54	A Fiber Bending Vector Sensor Based on M-Z Interferometer Exploiting Two Hump-Shaped Tapers. IEEE Photonics Technology Letters, 2015, , 1-1.	2.5	27

#	Article	IF	CITATIONS
55	Reconfigurable and ultra-sensitive in-line Mach-Zehnder interferometer based on the fusion of microfiber and microfluid. Applied Physics Letters, 2015, 106, 084103.	3.3	17
56	Mach–Zehnder Interferometer Based on S-Tapered All-Solid Photonic Bandgap Fiber. IEEE Photonics Technology Letters, 2015, 27, 1849-1852.	2.5	4
57	Polarization Rotator Based on Hybrid Plasmonic Photonic Crystal Fiber. IEEE Photonics Technology Letters, 2014, 26, 2291-2294.	2.5	6
58	Design for a Single-Polarization Photonic Crystal Fiber Wavelength Splitter Based on Hybrid-Surface Plasmon Resonance. IEEE Photonics Journal, 2014, 6, 1-9.	2.0	10
59	Real time and simultaneous measurement of displacement and temperature using fiber loop with polymer coating and fiber Bragg grating. Review of Scientific Instruments, 2014, 85, 075002.	1.3	8
60	Microfiber-Enabled In-line Fabry–Pérot Interferometer for High-Sensitive Force and Refractive Index Sensing. Journal of Lightwave Technology, 2014, 32, 1682-1688.	4.6	50
61	A novel all-fiber micro-displacement sensor based on long period grating and tip structure. Optoelectronics Letters, 2014, 10, 176-179.	0.8	2
62	Simultaneous Force and Temperature Measurement Using S Fiber Taper in Fiber Bragg Grating. IEEE Photonics Technology Letters, 2014, 26, 309-312.	2.5	27
63	Compact Long Period Fiber Grating Based on Periodic Micro-Core-Offset. IEEE Photonics Technology Letters, 2013, 25, 2111-2114.	2.5	23
64	Asymmetrically Corrugated Long-Period Gratings by Burning Fiber Coating and Etching Cladding. IEEE Photonics Technology Letters, 2013, 25, 1961-1964.	2.5	14
65	Long-Period Fiber Grating Cascaded to an S Fiber Taper for Simultaneous Measurement of Temperature and Refractive Index. IEEE Photonics Technology Letters, 2013, 25, 888-891.	2.5	93
66	Ultrasensitive Refractive Index Sensor Based on Microfiber-Assisted U-Shape Cavity. IEEE Photonics Technology Letters, 2013, 25, 1815-1818.	2.5	33
67	Two-dimensional bending vector sensing based on spatial cascaded orthogonal long period fiber. Optics Express, 2012, 20, 28557.	3.4	72
68	Highly Sensitive In-Fiber Refractive Index Sensor Based on Down-Bitaper Seeded Up-Bitaper Pair. IEEE Photonics Technology Letters, 2012, 24, 1878-1881.	2.5	27
69	Fiber-optic bending vector sensor based on Mach–Zehnder interferometer exploiting lateral-offset and up-taper. Optics Letters, 2012, 37, 4480.	3.3	151
70	Design of Broadband Single-Polarization Single-Mode Photonic Crystal Fiber Based on Index-Matching Coupling. IEEE Photonics Technology Letters, 2012, 24, 452-454.	2.5	15
71	Orthogonal Single-Polarization Single-Core Photonic Crystal Fiber for Wavelength Splitting. IEEE Photonics Technology Letters, 2012, 24, 1304-1306.	2.5	24
72	Controlled-Xgate with cache function for one-way quantum computation. Physical Review A, 2012, 85, .	2.5	2

#	Article	IF	CITATIONS
73	Characteristic analysis of a novel F-P interferometer based on a pair of FBGs with built-in LPFGs. Optoelectronics Letters, 2012, 8, 84-88.	0.8	2
74	Design and fabrication of period interlaced ULPG that inhibit specific resonance peaks. Microwave and Optical Technology Letters, 2011, 53, 1470-1472.	1.4	1
75	Design of supercontinuum source for coherent anti-Stokes Raman scattering microscopy. Optoelectronics Letters, 2008, 4, 103-105.	0.8	1
76	Light intensity-referred and temperature-insensitive fiber Bragg grating dynamic pressure sensor. Frontiers of Optoelectronics in China, 2008, 1, 113-118.	0.2	2
77	Statistical Neural Networks Based Blind Deconvolution of Spectroscopic Data. , 2007, , .		Ο
78	Method of correlation function for analyzing cross-sensitivity of strain and temperature in fiber grating sensors. Optoelectronics Letters, 2007, 3, 195-198.	0.8	8
79	Large Anomalous Dispersion at Short Wavelength and Modal Properties of a Photonic Crystal Fiber With Large Air Holes. IEEE Journal of Quantum Electronics, 2006, 42, 961-968.	1.9	11
80	An embedded FBG sensor for simultaneous measurement of stress and temperature. IEEE Photonics Technology Letters, 2006, 18, 154-156.	2.5	100
81	Temperature-insensitive fiber Bragg grating force sensor via a bandwidth modulation and optical-power detection technique. Journal of Lightwave Technology, 2006, 24, 3797-3802.	4.6	23
82	Illumination Variation in Images in Independent Component Analysis and Principal Component Analysis Subspaces. , 2006, , .		0
83	Fabrication of Dual-Wavelength Fiber Bragg Grating with a Longitudinal Stretch. Frontiers of Physics in China, 2006, 1, 108-111.	1.0	4
84	Reflection spectra of fiber Bragg gratings in quadratic strain field. Optoelectronics Letters, 2006, 2, 419-421.	0.8	0
85	Improving dynamic response of a temperature-only FBG sensor. Optoelectronics Letters, 2006, 2, 101-103.	0.8	1
86	Wide wavelength-switched optical-pulse generation in an L-band mode-locked erbium-doped fiber laser. Microwave and Optical Technology Letters, 2005, 44, 196-199.	1.4	3
87	A novel dual-wavelength fiber Bragg grating. Microwave and Optical Technology Letters, 2005, 44, 385-388.	1.4	0
88	Multi-wavelength erbium-doped fiber laser based on a microstructure fiber Bragg grating. Microwave and Optical Technology Letters, 2005, 46, 162-164.	1.4	3
89	Principles and realizations of FBG wavelength tuning with elastic beams. Optoelectronics Letters, 2005, 1, 5-9.	0.8	9
90	Gazing-detection of human eyes based on SVM. Optoelectronics Letters, 2005, 1, 65-68.	0.8	1

#	Article	IF	CITATIONS
91	A new setup to tune the center wavelength of FBGs. Optoelectronics Letters, 2005, 1, 107-109.	0.8	0
92	Applying Hopfield neural network to QoS routing in communication network. Optoelectronics Letters, 2005, 1, 217-220.	0.8	0
93	Strain-tuned dual-wavelength erbium-doped fiber laser. Microwave and Optical Technology Letters, 2004, 42, 323-324.	1.4	3
94	Temperature compensation for micro-vibration sensor with fiber gratings. Microwave and Optical Technology Letters, 2004, 42, 474-476.	1.4	2
95	Beating Frequency Tunable Dual-Wavelength Erbium-Doped Fiber Laser With One Fiber Bragg Grating. IEEE Photonics Technology Letters, 2004, 16, 1453-1455.	2.5	17
96	Pulse-Amplitude Equalization in a Rational Harmonic Mode-Locked Fiber Laser Using Nonlinear Modulation. IEEE Photonics Technology Letters, 2004, 16, 1813-1815.	2.5	19
97	Temperature-independent FBG-type torsion sensor based on combinatorial torsion beam. IEEE Photonics Technology Letters, 2002, 14, 1154-1156.	2.5	44
98	FBC-type sensor for simultaneous measurement of force (or displacement) and temperature based on bilateral cantilever beam. IEEE Photonics Technology Letters, 2001, 13, 1340-1342.	2.5	120
99	QoS routing with inaccurate information based on Hopfield neural network. , 0, , .		0
100	Invariant image encoding in neural network for target recognition. , 0, , .		0